Energy, Mines and Resources Canada
Énergie, Mines et Ressources Canada

CANMET
Canada Centre for Mineral and Energy Technology
Centre canadien de la technologie des minéraux et de l'énergie

PHASE CHARACTERISTICS AND MICROSTRUCTURES OF FURNACE SLAG DEPOSITS FROM A PILOT-SCALE RESEARCH BOILER FIRED WITH WESTERN CANADIAN THERMAL COALS

T.T. Chen, D.H.H. Quon and S.S.B. Wang
Mineral Processing Laboratory

January 1983

This document is an interim report prepared for the Mineral (CANMET)

Ce document est un rapport intérimaire préparé à l'intention du Centre canadien de la technologie des minéraux et de l'énergie (CANMET)

Project ERP-4.3.0.7.02
Low Grade Coal in Utility Boilers

35 pp

ENERGY RESEARCH PROGRAM
MINERAL SCIENCES LABORATORIES
DIVISION REPORT ERP/MSL 83-12(IR)

FEB 28 1984
MICROMEDIA

PHASE CHARACTERISTICS AND MICROSTRUCTURE OF FURNACE SLAG DEPOSITS FROM A PILOT-SCALE RESEARCH BOILER FIRED WITH WESTERN CANADIAN THERMAL COALS

by

T.T. Chen*, D.H.H. Quon*, and S.S.B. Wang*

ABSTRACT

The microstructure and composition of seven slag samples produced during combustion trials of Western Canadian thermal coals in a pilot scale utility boiler of the Canadian Combustion Research Laboratory were characterized, using optical and scanning electron microscopy, electron microprobe analysis and X-ray diffraction. Much of the slag deposit is composed of porous glassy aluminosilicate materials. Trace amounts of unmelted or recrystallized mullite, cristobalite, quartz and iron oxide are embedded in the matrix of glass. The major chemical constituents of the glass matrix are Al_2O_3 (20-34%) and SiO_2 (57-68%); minor and trace constituents are FeO (1.7-8.8%), K_2O (1.2-5.0%), CaO (1.2-4.1%), MgO, BaO, TiO_2 and P_2O_5. The composition of the matrix varies from spot to spot, and an increase of silica is usually compensated by a decrease of alumina. There is no systematic compositional variation inward from the furnace wall. The correlation between composition and microstructure requires consideration of the multicomponent phase equilibrium system; it is noted that the slags with lower Al_2O_3, higher FeO, CaO and/or K_2O tend to develop more glass.

---

* Mineral Sciences Laboratories, CANMET, 555 Booth Street, Ottawa, Ontario Canada, K1A 0G1.

CARACTERISTIQUES DE PHASE ET MICROSTRUCTURE DES SCORIES PROVENANT DE LA CHAMBRE DE CHAUFFE D'UNE CHAUDIERE PILOTE EXPERIMENTALE EXMPLOYANT DES CHARBONS THERMIQUES CANADIENS

par

T.T. Chen*, D.H.H. Quon*, et S.S.B. Wang*

RESUME

On a défini, pour une chaudière pilote expérimentale, productrice d'électricité, du Laboratoire canadien de recherche sur la combustion, la microstructure et la composition de sept échantillons de scories produites pendant des essais de combustion de charbons thermiques canadiens de l'Ouest; pour cela, on a fait appel aux méthodes du microscope optique et du microscope électronique à balayage, à l'analyse par microsonde électronique et à la diffraction des rayons X. En grande partie, les dépôts de scories sont composés d'aluminosilicates vitreux. Des quantités en traces de mullite, cristobalite, quartz et oxyde de fer recristallisées ou n'ayant pas subi la fusion sont encastrées dans la matrice vitreuse. Les principaux constituants chimiques de la matrice vitreuse sont Al_2O_3 (20-34 %) et SiO_2 (57-68 %); les constituants mineurs et en traces sont FeO (1,7-8,8 %), K_2O (1,2-5,0 %) CaO (1,2-4,1 %), MgO, BaO, TiO_2 et P_2O_5. La composition de la matrice varie d'un endroit à l'autre, et une augmentation de la concentration de silice est généralement compensée par une diminution de la concentration d'aluminium. On n'observe pas de variation systématique de la composition vers l'intérieur à partir de la paroi de la chambre de chauffe. La corrélation entre la composition et la microstructure exige

que l'on examine le système d'équilibre des phases, à composantes multiples; on remarque qu'avec les scories ayant moins d'Al_2O_3, et plus de FeO, CaO ou K_2O, et CaO et K_2O, il tend à se former plus de verre.

* Laboratoires des sciences minérales, CANMET, 555, rue Booth, Ottawa, Ontario K1A 0G1.

INTRODUCTION

Slagging and fouling of heat-transfer surface can be serious problems for utility boilers. The effects are: retardation of heat-transfer due to ash-deposition on heat-absorbing surfaces; increased shutdown of operations caused by rapid ash-deposition and formation of hard bonded deposits on convection surface; and corrosion/errosion of boilers due to deposition of alkali sulphates, chlorides and phosphates, etc. Study of composition, phases and structural characteristics of the ash deposits can provide valuable information for understanding the slagging and fouling processes in boilers.

As part of the CANMET effort to study the mechanism of slagging and fouling, seven furnace slag deposits from a pulverized coal-fired research boiler were examined to determine the composition, phase characteristics and microstructure. The results are presented in this report.

SAMPLES

The furnace slags examined were provided by the Canadian Combustion Research Laboratory (CCRL) of CANMET. The samples were generated in 1981 from the CCRL pilot scale boiler during firing Western Canadian thermal coals. The thermal behaviour ash melting characteristics (ASTM standard test) and the bulk chemical compositions (XRF analysis) of these samples given in Table 1 were also provided by CCRL.

In brief, slag A464/81 was produced during firing of a slightly oxidized, medium-volatile bituminous coal. The raw parent coal containing approximately 30% ash was cleaned to approximately 16% ash, prior to firing. Slag A484/81 was produced from the same 16% ash coal but fired under different excess air conditions. Slag A571/81 was obtained during firing of a 11% ash coal from the same parent coal.

Slag A592/81 was produced during firing a medium-volatile bituminous coal, with approximately 15% ash, while slag A613/81 was produced from the same coal under different firing conditions, i.e., excess air.

Both slag A519/81 and slag A545/81 were produced from low-volatile bituminous coal, with approximately 20% ash, but fired under different conditions, i.e., excess air.

ANALYTICAL METHODS

Both polished sections and thin sections of the as received slag samples were prepared. The samples were then characterized using X-ray diffraction (XRD), optical and scanning electron microscopy (SEM), and energy-dispersive X-ray analysis (EDX). The compositions of the phases were determined using an electron microprobe (EMP). Because the slags consist almost entirely of glass, individual spot compositions do not appear to be significant. The homogeneity of the glass was examined using EDX and backscattered electron images (BSE) from the SEM, in which the homogeneity of the composition was expressed as the homogeneity of the BSE image.

In order to examine the localized or gradational compositional changes in the sample, a small cross-section of the sample from near the boiler wall (i.e., an early deposition) to the inner of boiler (i.e., a late deposition) was analyzed systematically using EMP and SEM. As to be expected, the area actually examined by the microbeam techniques represents only a small portion of the total sample. However, the techniques are still the most effective way to study the microstructure and the chemistry of the coal slags.

PHASE CHARACTERISTICS

Sample A464/81

Only crushed material was available for this study. The sample consists mainly of porous glass, with minor to trace amount of mullite $Al_6Si_2O_{13}$, Fe_3O_4, quartz and cristobalite embedded in the glass matrix. The composition of the glass varies slightly from spot to spot, primarily in the SiO_2 and Al_2O_3 content; the average electron microprobe analysis is: Al_2O_3 29.5, SiO_2 60.0, FeO* 2.6, MgO 1.1, BaO 0.5, TiO_2 1.8, K_2O 1.6, CaO 3.0, total 100.1 wt %. The general texture of the slag is shown in Fig. 1, where the major portion of the slag is composed of aluminosilicate glass, and slightly less than half of the total volume is pores. A slight variation of the composition in the glass is barely seen by the small difference in the brightness of the

---

* In this report, in all the electron microprobe analyses, Fe is calculated as FeO, and Na has not been determined.

image, where the darker areas contain more alumina. Quartz and cristobalite occur as small (approximately 10-15 μm) anhedral grains. Occasionally, a very small proportion of the slag contains spinel (Fe_3O_4), mullite, and Al-Ca-Fe silicate (Fig. 2); localized acicular mullite crystals are present as a densely packed mass (Fig. 3); spinel occurs as crystal aggregates, and the Al-Ca-Fe silicate occurs as dendrites dispersed in the glass matrix. Trace amounts of Fe_2O_3 and graphite are also observed.

Sample A484/81

This sample is porous, loosely bonded, and is fine-grained* and light grey** in color on the outer surface (Fig. 4), but grades into coarse-grained and light yellowish brown in the innter portion (Figs. 5,6,7). A poorly defined layer structure parallel to the slag surface is also evident.

The sample consists mainly of glass with minor to trace amounts of mullite (acicular crystals), cristobalite, quartz (subrounded to irregular masses), iron oxides (spherules, irregular grains; Fig. 8) and Al-Ca-Fe-Ti-K silicate (dendrites) embedded in the matrix of glass. The composition of the glass varies from spot to spot, with an average electron microprobe analysis of: Al_2O_3 27.4 (20.1-33.6), SiO_2 60.4 (57.4-67.2), FeO 2.7 (1.7-3.7), MgO 1.0 (0.7-1.3), BaO 0.7 (0.6-0.8), TiO_2 1.6 (1.2-2.2), P_2O_5 0.7 (0.4-1.1), K_2O 2.4 (1.7-3.1) and CaO 2.9 (2.0-4.1), total 99.8 wt %. The variation of the composition from the outer surface to the inner portion (near boiler wall) of the slag is shown in Fig. 9, their corresponding analyses are given in Table 2, where each analysis represents an area of approximately 0.005 mm^2. The variations in Al_2O_3 and SiO_2 is particularly noticeable, as the variation can be as high as 50% within a distance of a few micrometres. As can be seen from this figure, the variation of composition is random except that wherever an increase of Al_2O_3 occurs, there is a corresponding decrease of SiO_2.

The textures, from the outer surface to the inner portion of the slag, shown in Figs. 10, 11 and 12, are essentially similar; the detailed structure is shown in Fig. 13 (enlargement of the upper-left portion of

---

* Each small blob or lump is referred here as a grain.

** The ISCC-NBS (Inter-Society Colour Council - National Bureau of Standard) colour-name is used in this report (see Supplement to NBS Circular 553).

Fig. 12). The figure shows that the main structure (matrix) is aluminosilicate glass. Quartz and cristobalite occur as anhedral grains; mullite occurs as fine irregular clusters, as rims surrounding quartz grains, or as sub-rounded aggregates embedded in the glass matrix.

Sample A571/81

The sample is similar to sample A484/81, showing "sintered" and "loosely bonded" textures. The surface is light grey and relatively dense (Fig. 14), and the cross-section is yellowish grey to greyish yellow brown, and uniformly porous (Fig. 15).

The main constituent of the sample is glass, with trace amounts of mullite (spherules), cristobalite and quartz dispersed in the glass matrix. Feldspar and graphite were also detected by XRD in trace amounts. The composition of the glass (containing major amounts of Al, Si, minor Ca, Fe, Ti, and trace amounts of K, Mg and Ba) varies slightly, and shows no apparent difference between the inner (near boiler wall) and the near surface portion of the slag sample. However, the inner portion (Figs. 15,16) appears to contain more crystalline phases (such as, quartz, cristobalite and mullite) than the outer portion (Figs. 14,17).

Sample A592/81

The surface ("liquid surface") of the slag sample is light grey. The colour is primarily due to contamination by dust and fly ash, such as iron oxide spherules. The surface is relatively compact, containing relatively smaller pores (Fig. 18), while the cross-section is uniform with large pores being distributed in the glass matrix (Figs. 19,20). The colour of the cross-section varies from yellowish grey to light olive grey or light greyish olive. In comparison with the previous samples (A464, A484 and A571), this sample is olive in colour, has larger pores, and is more glassy, presumably due to its lower fusion temperature and higher volatile content (Table 1).

In addition to the principal glass phase, trace amounts of mullite and quartz were found dispersed in the matrix of glass. Occasionally, local concentrations of iron oxide (spherules or irregular grains), mullite, Mg-Al-Ca silicate, TiO_2, and Ca-Al silicate were also observed (Fig. 21). The composition of the glass is mainly aluminosilicate, with minor amounts of Ca, Fe and K, and trace amounts of Ti, Mg and Ba. The chemical composition varies

from spot to spot (Fig. 18). Variation as high as 50% in silica and alumina was observed within a distance of a few micrometres. However, there is no systematic gradient in any component from the inner to the outer portion of the slag deposit (Fig. 2?; Table 3) apart from the inverse relation between SiO_2 and Al_2O_3. The average composition gives: Al_2O_3 23.4 (18.5-31.4), SiO_2 64.4 (57.9-68.6), FeO 4.8 (4.2-5.2), MgO 1.2 (1.0-1.4), BaO 0.3 (0.3-0.4), TiO_2 0.9 (0.8-1.1), K_2O 3.0 (2.5-3.3), CaO 2.9 (2.0-3.5), total 100.9 wt %.

Sample A613/81

Only crushed material was available for this study. The sample is light pale yellowish green. Trace amounts of mullite, quartz (subrounded grains) and Fe_7Si_3 (spherules; Si 16.4, Fe 81.3, P 2.1 wt %) were observed in the matrix of glass (Fig. 23). The composition of the glass (major Al, Si, minor Ca, K, Fe and trace Ti, Ba, Mg) is relatively uniform, showing small variations in Si, Al, Ca and Fe. The average composition (EMP analysis) is: SiO_2 67.5, Al_2O_3 21.9, FeO 2.5, MgO 1.4, BaO 0.6, TiO_2 1.2, K_2O 1.4 and CaO 2.6, total 99.1 wt %.

Sample A519/81

This sample is different from the previous samples, with more Fe, K, and less Al and Ca (Table 4). A change in colour over the cross-section is noticeable, with the surface being brownish grey, and grading into olive grey within a few millimetres of the surface, the centre portion is greyish green yellow, while the inner portion (adjacent to boiler wall) is dark greyish brown to greyish brown. The pore sizes are variable, but, in general still maintain a homogeneous appearance throughout the cross-section (Figs. 24,25).

The sample is mainly glass. Trace amounts of mullite and quartz occurs as small spherical grains dispersed in the matrix of glass. The composition of the glass varies from spot to spot as indicated in Fig. 26, where the darker areas contain higher Al_2O_3, and compositional changes usually occur within a short distance. Table 4 is a summary of the analyses obtained by scanning from the outer surface to the inner portion of the slag deposit; each analysis represents an area of approximately 0.005 mm^2, and each area is approximately 5 mm apart. A total of 17 analyses covers a scanning distance of approximately 75 mm. The results are also graphically presented in Fig. 27. Again, it shows the random variation of the sample composition, and the

negative correlationship between alumina and silica. The average composition of the glass is: Al_2O_3 20.6 (17.9-24.5), SiO_2 62.6 (61.1-64.5), FeO 7.3 (5.1-8.8), MgO 1.4 (1.1-1.8), BaO 0.4 (0.4-0.5), TiO_2 0.8 (0.8-1.1), P_2O_5 0.9 (0.6-1.2), K_2O 4.6 (4.1-5.0), CaO 1.3 (1.2-1.5), total 99.9 wt %.

In addition to the block fragment described above, a crushed sample was also available for this study. In the crushed particles, local concentrations of iron oxide, quartz, and mullite were observed (Fig. 28). The iron oxide (presumably Fe_2O_3) occurs as spherical aggregates of euhedral crystals (Fig. 29); quartz occurs as subrounded grains; and mullite occurs as needle-like aggregates. The particles probably represent the surface portion (outermost shell) of the slag which are contaminated by fly ash.

Sample A545/81

This sample is similar to A519/81 in composition, colour and porosity. The general texture is shown in Figs. 30, 31 and 32, the heterogeneity of the glass composition is shown in Fig. 33.

DISCUSSION

The slag samples studied consist almost entirely of porous glass. Trace amounts of mullite, quartz, cristobalite and iron oxide are dispersed in the glass matrix. The tendency for mullite to crystallize as needle crystals, quartz and cristobalite to occur as anhedral grains, and iron oxides to form subhedral to euhedral crystal-aggregates indicates that these phases are either unmelted or recrystallized at high temperature, or are crystallized during rapid cooling from the melt.

The main constituents of the glass matrix are silica and alumina, with minor to trace amounts of Fe, Ca, Mg, Ti, Ba, K, Na and P. The composition of the glass varies from spot to spot. Particularly noticeable is the alumina and silica content, variation as great as 50% can be observed within a distance of a few micrometres. There is no systematic compositional gradient from the outer surface to the inner portion (near boiler wall) of the slag deposit, except that wherever an increase of alumina occurs, there is a decrease of silica. The relationship is apparent, as the slag is mainly of aluminosilicate composition (Al_2O_3 + SiO_2 ≈90%; A484/81, A592/81), an increase

of Al_2O_3 requires a decrease in SiO_2 to satisfy the mass balance restriction. For the lower aluminosilicate slag such as A519/81 where (Al_2O_3 + SiO_2) ≈83%, the relationship is less perfect. The high proportion of Al_2O_3 and SiO_2 in these samples presumably indicates that the mineral matter in the original coal is mainly of aluminosilicates and that most of the alkalies in the mineral matter has been lost through volatilization during melting of the ash. The observed negative correlationship between silica and alumina is different from that observed by Fessler et al. (1980), who found that an increase of Al_2O_3 was accompanied by an increase of SiO_2 (and also K_2O) in the melt/ash as a result of the major constituent of illite in their initial ash. As their melt/ash is relatively low in aluminosilicate (Al_2O_3 + SiO_2 ≈70%) and their ash is only partially fused, most of the original constituents in the mineral matter still remained in the melt/ash; consequently, for parental ash rich in illite (K-Al silicate), an increase of alumina in the melt is likely to be accompanied by an increase of silica (and also K_2O).

Some of the slags are more glassy and porous (e.g., A592/81, A519/81, A613/81) whereas the others are relatively "sintered and loosely-bonded" in texture (e.g., A464/81, A484/81, A571/81). The glassy and highly porous texture is found in material with a lower fusion temperature, whereas the "sintered and loosely-bonded" texture is observed in material with a higher fusion temperature (Table 1).

As has been reported elsewhere, the ash-fusion temperature can be correlated with the phase diagrams of SiO_2 - Al_2O_3 - XO, where X = Fe, Ca or K_2 (Huffmann et al. 1981; Huggins et al. 1981). In general, the ash-fusion curve parallels with the liquidus of the phase diagram except for, in some cases, a lowering of ash-fusion temperatures and a shifting of pseudoeutectic composition due to the effect of other minor elements (Huggins et al. 1981). The compositions of the slags (glass matrix) studied generally fall within the mullite fields (SiO_2 75-82, Al_2O_3 15-22 mole %)* of the ternary diagrams of Al_2O_3-SiO_2-FeO, Al_2O_3-SiO_2-CaO, and Al_2O_3-SiO_2-K_2O (Levin et al. 1964). An increase of Al_2O_3 in the composition means an increase of liquidus temperature (i.e., implying the decrease of ash-melting), whereas an increase of FeO, K_2O or CaO tends to decrease the liquidus temperature (i.e., the increase of ash

---

* Assuming SiO_2 + Al_2O_3 + FeO (or CaO, K_2O) = 100%

melting). For example, slag A519/81 (Al_2O_3 15.0, SiO_2 77.4, FeO 7.6 mole %) containing higher FeO and lower Al_2O_3 has lower fusion temperature, whereas slag A464/81 (Al_2O_3 21.8, SiO_2 75.5, FeO 2.7 mole %) containing lower FeO and higher Al_2O_3 has higher fusion temperature (Table 1). However, an increase of CaO from 1.8 of A519/81 to 4.0 mole % of A464/81 appears to have no effect on the fusion temperature as shown by the isotherms of the Al_2O_3-SiO_2-CaO phase diagram.

The minor constituents of the slag, such as Fe, Mg, K, Ca, Ba, Ti etc., are distributed mainly in the glass matrix, and the composition of the glass appears to show no correlation with the minor phases (such as, iron oxides, mullite, quartz and cristobalite, etc.) found in the samples. For example, slag A519/81 and A592/81 contain more Fe but fewer iron oxide inclusions in the glass matrix, while slag A464/81 and A484/81 have more Al and also more mullite inclusions in the glass. Obviously, the composition of the slag is inherited from the mineral matter of the original coal, while the concentrations of the minor phases in the glass matrix is affected by the degree of fusion.

The slag samples are highly porous, and approximately half of the total volume is occupied by pores. The porosity of the slag is caused by the entrapped gas in the melt at high temperature. Over the cross-section of the slag deposit, the size and distribution of the pores are random, but, generally retain a uniform appearance across the whole section, although at the surface ("liquid surface"), the size and porosity decrease, and this may be attributed to the surface tension of the melt.

ACKNOWLEDGEMENTS

The authors wish to thank H. Whaley and R. Prokopuk of the Canadian Combustion Research Laboratory for valuable discussions and for providing materials for this study, also J.M. Beaulne and J.Y. Bourgoin for preparation of polished sections.

REFERENCES

1. Fessler, R.R., Skidmore, A.J., Hazard, H.R. and Dimmer, J.P. "Composition and microstructure of a furnace ash deposit from a coal-fired utility boiler"; Journal Engineering for Power; Trans ASME; 102:692-697; 1980.

2. Huffman, G.P., Huggins, F.E. and Dunmyre, G.R. "Investigation of the high-temperature behaviour of coal ash in reducing and oxidizing atmospheres"; Fuel 60:585-593; 1980.

3. Huggins, F.E., Kosmack, D.A. and Huffman, G.P. "Correlation between ash fusion temperatures and ternary equilibrium phase diagrams"; Fuel 60:577-584; 1981.

4. Levin, E.M., McMurdie, H.F. and Hall, H.P. "Phase diagrams for ceramists"; Columbus, Ohio; American Ceramic Society; 1964.

Table 1 - Fusion temperatures and slag compositions

Fusion temperature °C	A464/81	A484/81	A571/81	A592/81	A613/81	A519/81	A545/81
Oxidizing atmosphere							
Initial deformation	1482 +	1482 +	1482 +	1316	1343	1343	1410
Softening	+	+	+	1438	1468	1482	1471
Hemispherical	+	+	+	1482 +	1482 +	1482 +	1482 +
Fluid	+	+	+	+	+	+	+
Reducing atmosphere							
Initial deformation	1482 +	1482 +	1482 +	1332	1310	1341	1341
Softening	+	+	+	1421	1474	1427	1443
Hemispherical	+	+	+	1482 +	1482 +	1482 +	1482 +
Fluid	+	+	+	+	+	+	+
Composition (XRF analyses; wt %)							
SiO_2	58.84	58.31	59.41	61.79	52.23	61.63	62.67
Al_2O_3	28.73	29.42	29.98	23.29	20.58	23.45	23.14
Fe_2O_3	2.83	2.33	2.36	2.87	3.02	6.57	5.87
TiO_2	1.45	1.53	1.35	0.97	0.94	0.96	0.51
P_2O_5	0.50	0.64	0.77	0.33	0.42	1.10	0.80
CaO	2.74	2.54	2.86	3.33	2.98	2.05	1.70
MgO	0.70	0.58	0.77	1.26	0.96	1.16	1.13
SO_3	0.30	<0.01	<0.01	0.14	<0.01	0.20	<0.01
Na_2O	0.10	0.11	0.14	0.76	0.71	0.08	0.09
K_2O	1.26	1.01	0.98	1.42	1.17	2.53	2.71
BaO	0.35	0.53	0.93	0.95	1.13	0.07	0.93
SrO	0.39	0.11	0.20	0.10	0.12	0.08	0.26
LOF	0.7	0.10*	0.3	1.84*	0.91*	<0.1	0.2
Total	98.89	97.22	100.06	99.05	85.18	98.73	100.02

+ Higher than 1482°C.

* Determined at Mineral Sciences Laboratories. All other data were provided by Canadian Combustion Research Laboratory.

Table 2 - Electron microprobe analyses of glass matrix in slag A484/81

	1	2	3	4	5	6	7	8	9	10	11	12	13	14
Al_2O_3	28.8	29.9	24.6	26.9	21.1	23.7	25.4	33.6	29.5	27.7	31.9	20.1	31.8	28.7
SiO_2	57.8	58.6	62.3	59.8	64.2	64.0	62.5	57.4	58.6	60.5	57.2	67.2	57.8	57.6
FeO*	3.7	2.9	2.3	3.3	3.1	2.6	3.0	1.7	2.5	2.2	2.5	3.2	2.3	2.9
MgO	1.3	0.8	1.1	1.1	1.1	1.2	0.9	0.8	0.7	0.9	1.0	1.0	0.9	1.0
BaO	0.8	0.6	0.8	0.6	0.8	0.7	0.8	0.8	0.7	0.8	0.6	0.6	0.6	0.8
TiO_2	1.7	1.2	1.8	1.3	1.6	1.3	2.2	1.6	1.7	1.6	1.8	1.4	1.3	1.6
P_2O_5	0.7	0.4	0.8	0.8	0.8	0.8	0.7	0.5	0.7	1.1	0.6	0.4	0.8	0.9
K_2O	1.7	2.3	2.3	2.1	2.4	2.1	2.1	2.0	2.5	2.9	2.6	3.1	2.7	2.7
CaO	2.8	2.0	4.1	2.9	3.5	2.6	2.7	2.3	2.7	3.6	2.7	2.8	2.7	3.8
Total	99.3	98.7	100.1	98.8	98.6	99.0	100.3	100.7	99.6	101.2	100.9	99.8	100.9	100.0

* Fe calculated as FeO.

The analyses are listed in order of increasing distance from the slag surface ("liquid surface"), i.e., No. 1 is near the surface, and No. 14 is the innermost (near boiler wall), with the total distance from No. 1 to No. 14 approximately 18 mm.

Table 3 - Electron microprobe analyses of glass matrix in slag A592/81

	1	2	3	4	5	6	7	8	9	10	11	12	13	14	15	16	17	18
Al_2O_3	31.4	21.0	21.7	24.8	25.2	23.5	22.6	25.6	23.0	22.4	22.9	20.8	26.2	21.6	20.4	26.4	18.5	23.2
SiO_2	57.9	65.1	65.2	63.6	62.7	64.9	64.9	62.4	65.1	66.5	64.5	67.0	62.3	64.9	67.4	61.4	68.6	64.8
FeO*	4.8	4.8	4.5	4.9	5.0	5.0	5.1	4.9	4.3	4.3	5.2	4.4	5.0	5.1	4.7	4.9	4.9	4.9
BaO	0.3	0.3	0.3	0.3	0.3	0.3	0.4	0.3	0.4	0.3	0.3	0.3	0.3	0.4	0.4	0.3	0.4	0.4
MgO	1.0	1.2	1.1	1.3	1.0	1.3	1.1	1.3	1.2	1.2	1.4	1.4	1.2	1.3	1.1	1.4	1.2	1.1
TiO_2	1.0	1.0	1.0	0.8	0.8	0.9	1.0	0.9	0.9	1.0	0.9	0.9	1.0	0.9	0.9	1.0	1.0	1.0
K_2O	2.5	2.9	3.2	3.2	3.2	2.9	2.7	3.0	3.1	3.2	3.2	3.2	3.2	3.1	3.0	3.2	3.0	3.2
CaO	2.8	2.9	3.3	3.0	2.4	2.0	2.4	3.5	3.1	3.2	2.8	2.8	3.0	3.1	2.6	2.6	3.6	3.5
Total	101.7	99.2	100.3	101.9	100.6	100.8	100.2	101.9	101.1	102.1	101.2	100.3	102.2	100.4	100.5	101.2	101.2	102.3

* Fe calculated as FeO.

The analyses are listed in order of increasing distance from the slag surface, with No. 1 closest to the slag surface and No. 18 closest to the boiler wall. The total distance from No. 1 to No. 18 is approximately 64 mm.

Table 4 - Electron microprobe analyses of glass matrix in slag A519/81

	1	2	3	4	5	6	7	8	9	10	11	12	13	14	15	16	17
Al_2O_3	20.0	20.5	22.6	18.6	19.0	19.1	24.5	23.9	19.2	21.4	20.5	18.9	19.5	19.8	22.8	24.3	20.1
SiO_2	63.0	62.7	62.7	64.6	62.8	63.6	62.0	61.1	62.9	61.8	61.6	63.5	63.0	63.9	62.2	59.6	62.6
FeO*	6.9	7.7	6.4	8.5	7.7	7.7	5.8	7.0	7.6	8.0	7.7	8.8	7.9	7.0	5.1	5.4	7.1
MgO	1.4	1.7	1.4	1.8	1.5	1.5	1.2	1.5	1.3	1.7	1.6	1.6	1.1	1.3	1.4	1.1	1.2
BaO	0.4	0.4	0.4	0.4	0.4	0.4	0.4	0.4	0.4	0.4	0.4	0.4	0.4	0.5	0.5	0.4	0.5
TiO_2	0.8	0.8	0.8	0.8	0.9	0.8	0.8	0.9	0.9	0.8	0.8	0.8	0.8	1.0	0.9	0.9	0.9
P_2O_5	0.7	0.9	0.8	0.7	0.8	1.0	0.7	0.8	0.9	0.9	1.0	0.6	0.8	1.1	1.2	1.3	1.1
K_2O	4.6	4.6	4.8	4.8	4.9	4.7	4.5	4.3	4.4	5.0	5.0	4.7	4.7	4.8	4.1	5.0	4.3
CaO	1.2	1.2	1.4	1.4	1.4	1.2	1.5	1.2	1.5	1.4	1.3	1.1	1.2	1.7	1.4	1.9	1.5
Total	99.0	100.5	101.3	101.6	99.4	100.0	101.4	101.1	99.1	101.4	99.9	100.4	99.4	101.1	99.6	99.9	99.3

* Fe calculated as FeO.

The analyses are listed in order of increasing distance from the slag surface, with No. 1 closest to the slag surface and No. 17 closest to the boiler wall; the total distance from No. 1 to No. 17 is approximately 76 mm.

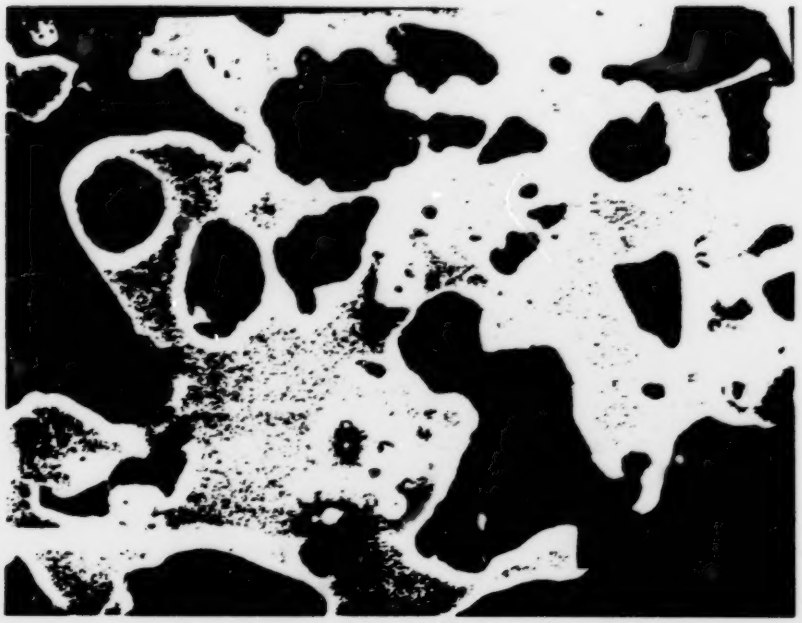

Fig. 1 - General texture of the slag A464/81 (BSE image), showing that the framework is mainly of glass, and that approximately less than half of the volume is voids. (The bright spots are holes contaminated by Pb due to polishing).

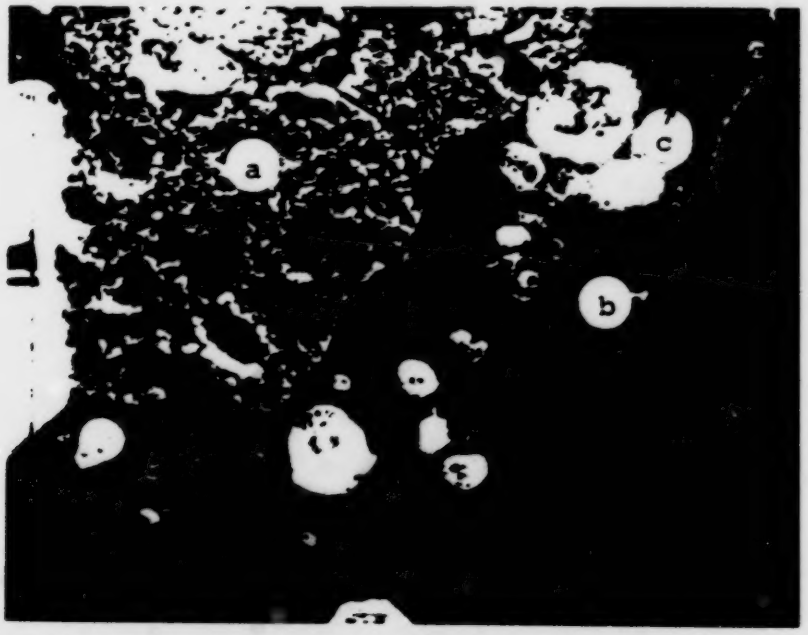

Fig. 2 - SEM photograph of a slag A464/81 fragment, showing euhedral Fe_3O_4 crystals (a), mullite aggregate (b), and dendritic Al-Ca-Fe silicate (c) in a matrix of aluminosilicate glass. (The bright spots are pores but contaminated by Pb due to polishing).

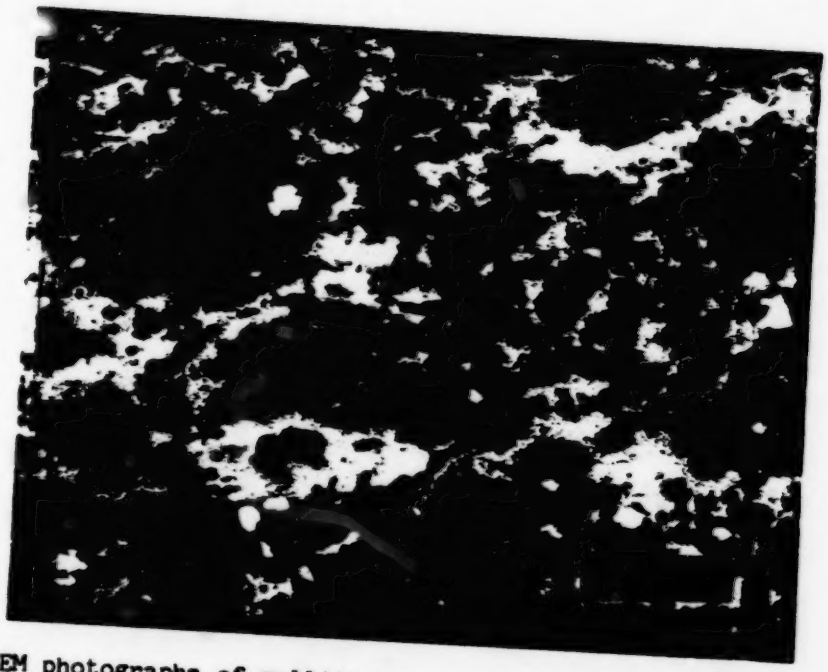

Fig. 3 - SEM photographs of mullite aggregate in slag A464/81.

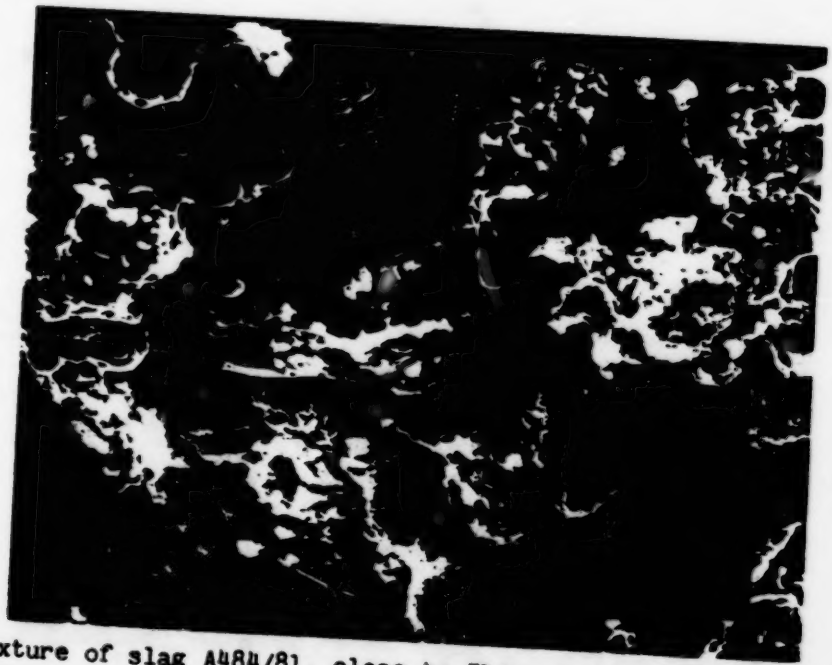

Fig. 4 - Texture of slag A484/81, close to "liquid surface" portion. In general, this portion is relatively denser and the blobs are finer in size.

Fig. 5 - Texture of the outer portion (cross-section, close to surface) of the slag A484/81. The slag is mainly of glass.

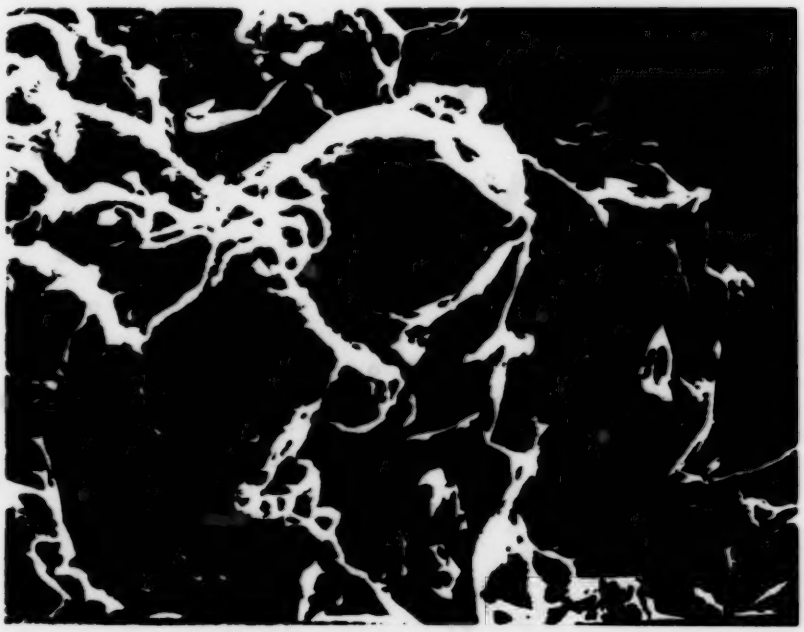

Fig. 6 - Texture of the middle portion (cross-section) of the slag A484/81.

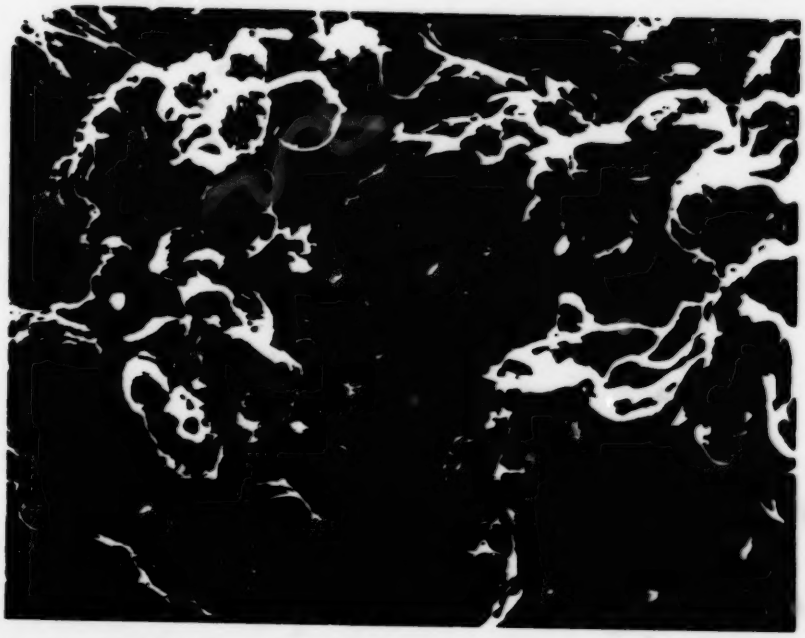

Fig. 7 - Texture of the inner portion (close to boiler wall; cross-section) of the slag A484/81.

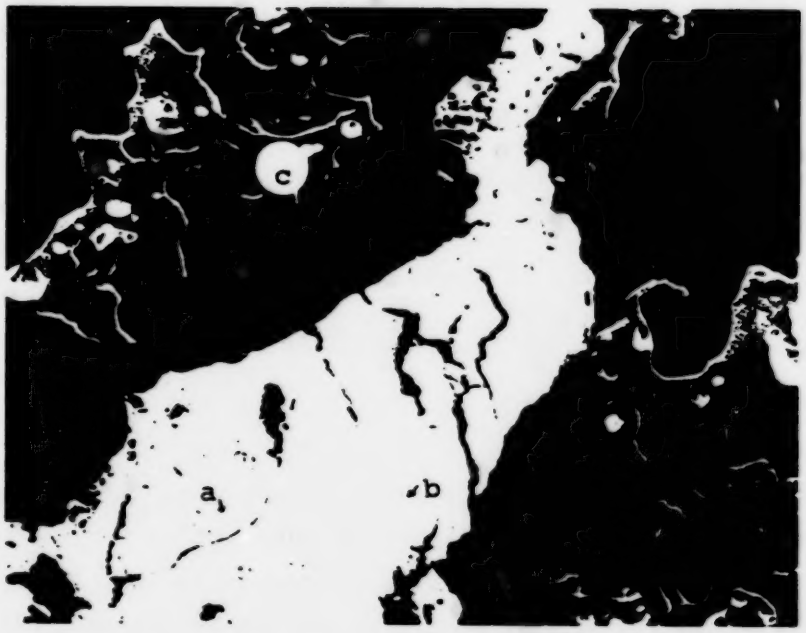

Fig. 8 - SEM photograph of fragments of slag A484/81, showing mixture of Fe_2O_3 (a) and Fe_3O_4 (b); the grey coloured grains are glass (c).

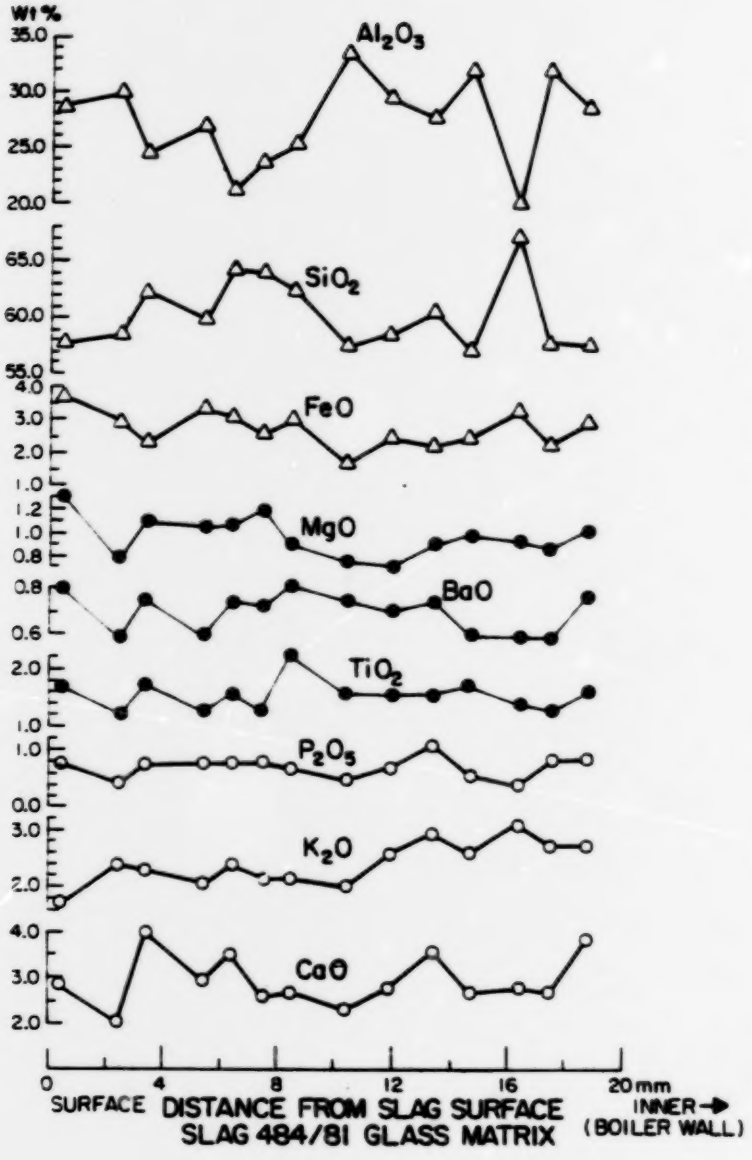

Fig. 9 - Compositional variation of glass matrix from the near surface ("liquid surface") portion to the inner portion (near boiler wall) of the slag A484/81. Each analysis represents an area of approximately 0.005 mm^2. (Al, Si and Fe), (Mg, Ba and Ti) and (K, Ca and P) were determined separately.

Fig. 10 - Texture of the outer portion (near "liquid surface") of the slag A484/81 (SEM photo).

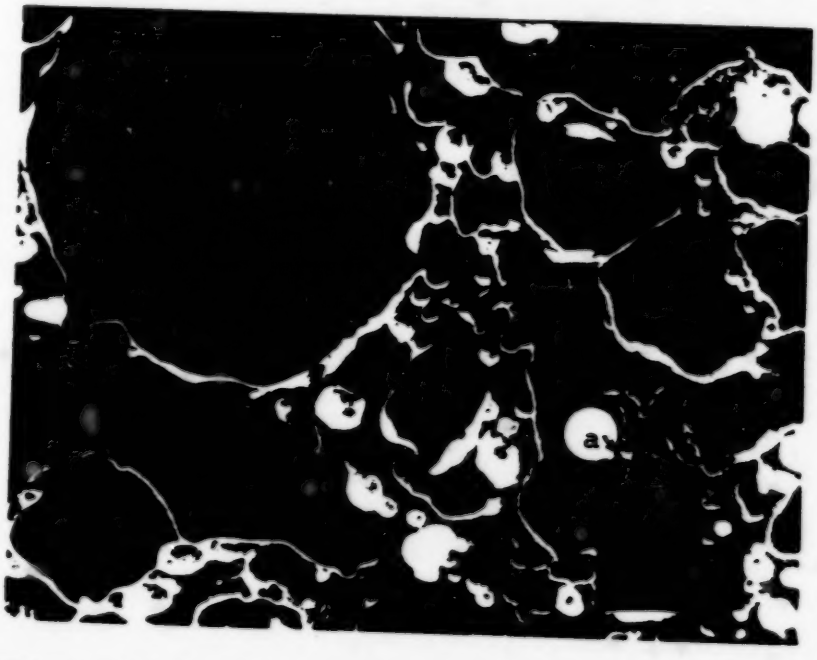

Fig. 11 - Texture of the middle portion of the slag A484/81 (SEM photo). The aggregates (a) are mixtures of SiO_2, mullite and glass.

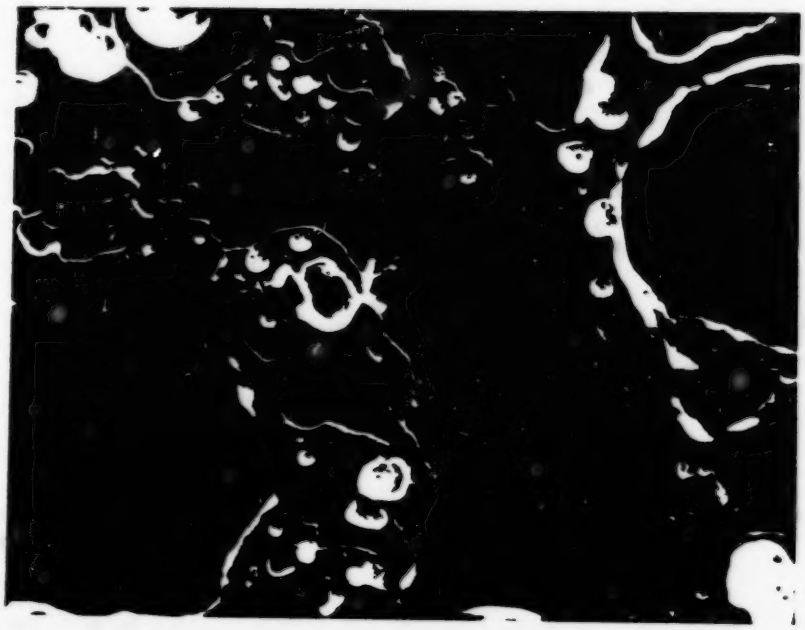

Fig. 12 - Texture of the inner portion (near boiler wall) of the slag A484/81 (SEM photo).

Fig. 13 - BSE image of slag A484/81 showing the details of the slag (corresponding to the upper-left quarter of Fig. 12). The main structure (a) is glass, the dark grains (b) are SiO_2, the fine irregular clusters (c) are mullite, the dark rim (d) surrounding SiO_2 grain is mullite, the subrounded aggregate (e) is mullite plus glass.

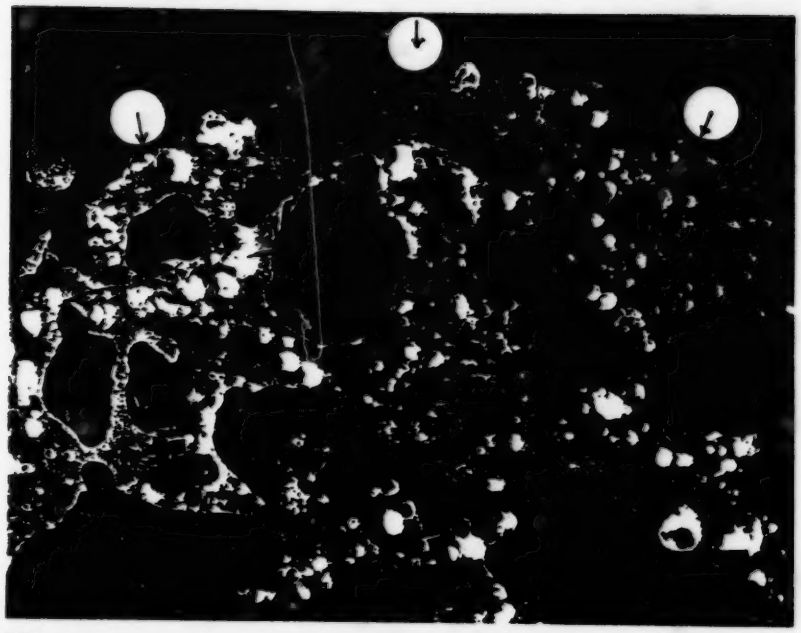

Fig. 14 - BSE image showing the general texture of the outermost portion (cross-section) of the slag A571/81. In comparison to the inner portion (Fig. 15), this portion is relatively dense. The original "liquid surface" is indicated by arrows. (The bright spots are pores but contaminated by Pb due to polishing).

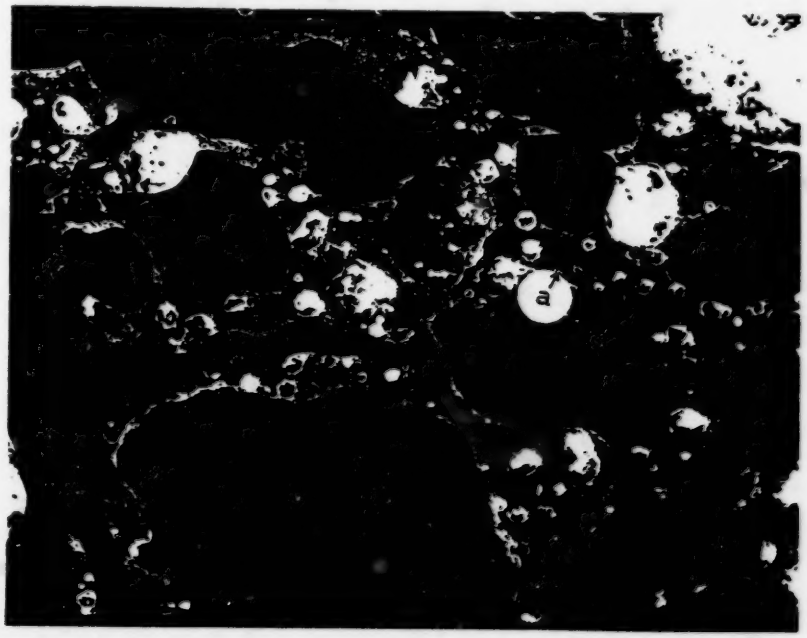

Fig. 15 - BSE image showing the general texture of the inner portion of the slag A571/81. The main structure is glass, the dark inclusions (a) are SiO_2.

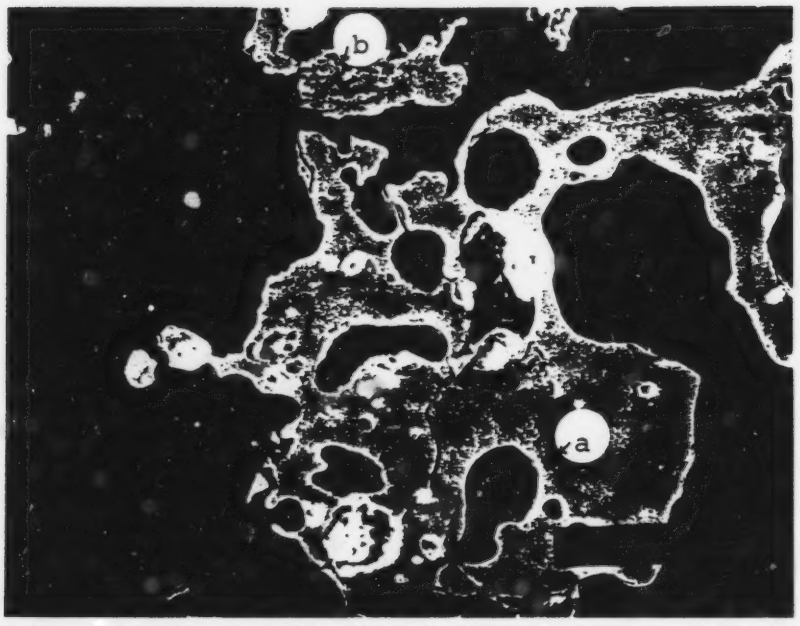

Fig. 16 - BSE image showing the details of the inner portion of the slag A571/81. The dark inclusions (a) are SiO_2, the pitty mass (b) is mullite. In comparison to the outer portion (Fig. 17), this portion appears to contain more mullite and SiO_2.

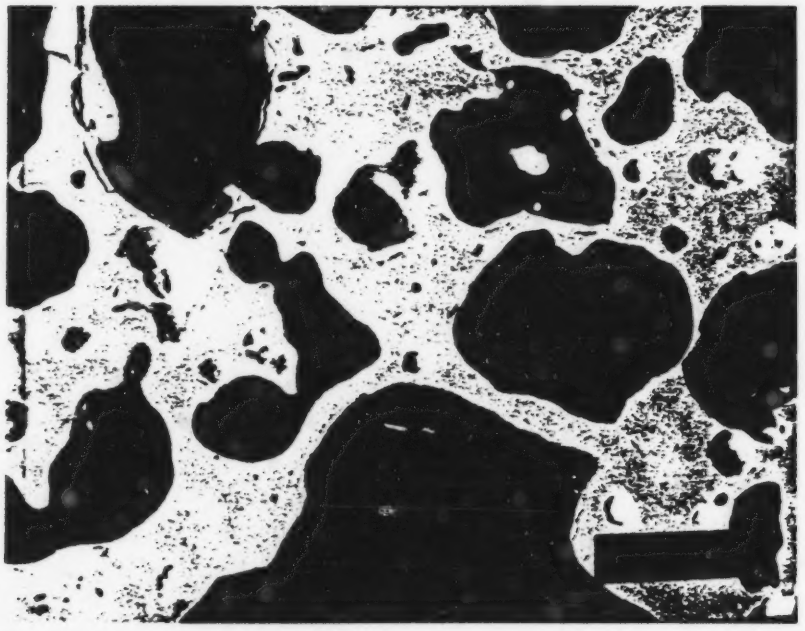

Fig. 17 - BSE image showing the details of the outer portion of the slag A571/81. The framework is glass.

Fig. 18 - BSE image of the outermost portion (within 1 mm from the surface) of the slag A592/81. In this portion, the slag is relatively compact; the heterogeneity of the glass composition is immediately evident, as indicated by the variation of the brightness of the image, the darker areas contain higher Al_2O_3.

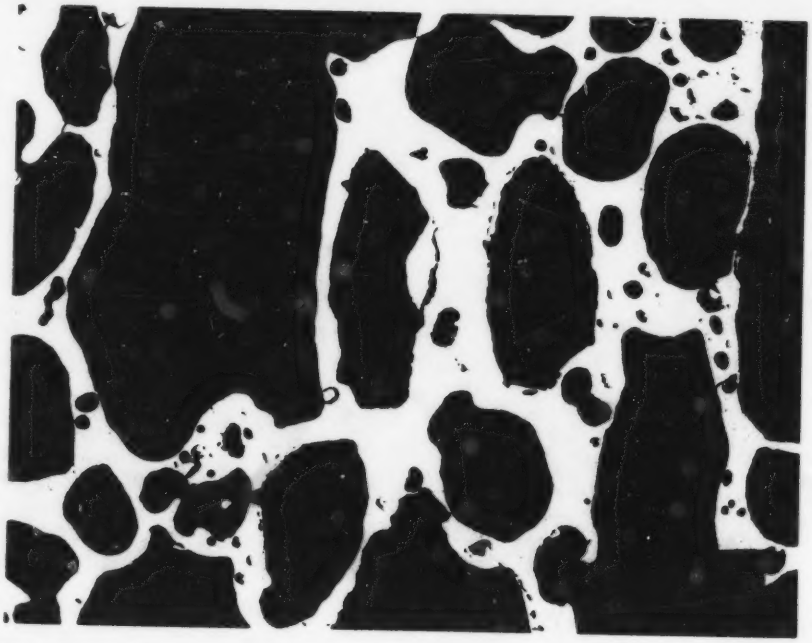

Fig. 19 - BSE image showing the general texture of the outer portion of the slag A592/81. Approximately two thirds of the volume is occupied by pores.

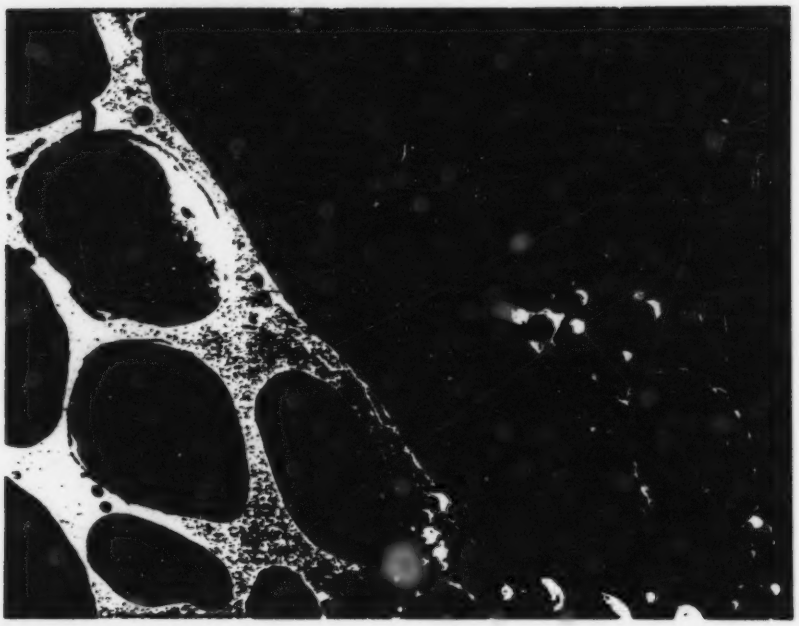

Fig. 20 - BSE image showing the general texture of the inner portion of the slag A592/81. The porous nature of the slag is evident.

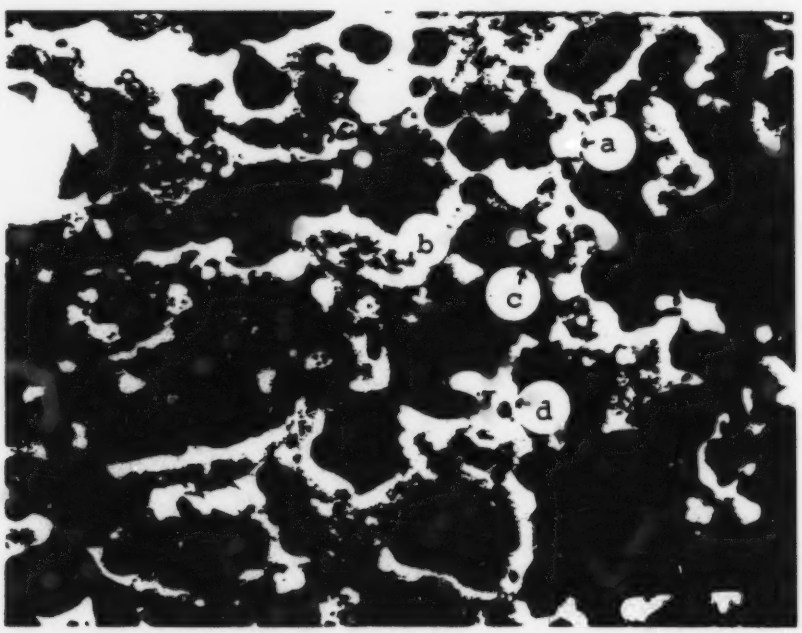

Fig. 21 - Secondary electron image of a brownish fragment of slag A592/81, showing the presence of abundant iron oxide (a), TiO_2 (b), SiO_2 (c), and Al-Ca silicate (d) in the glass matrix.

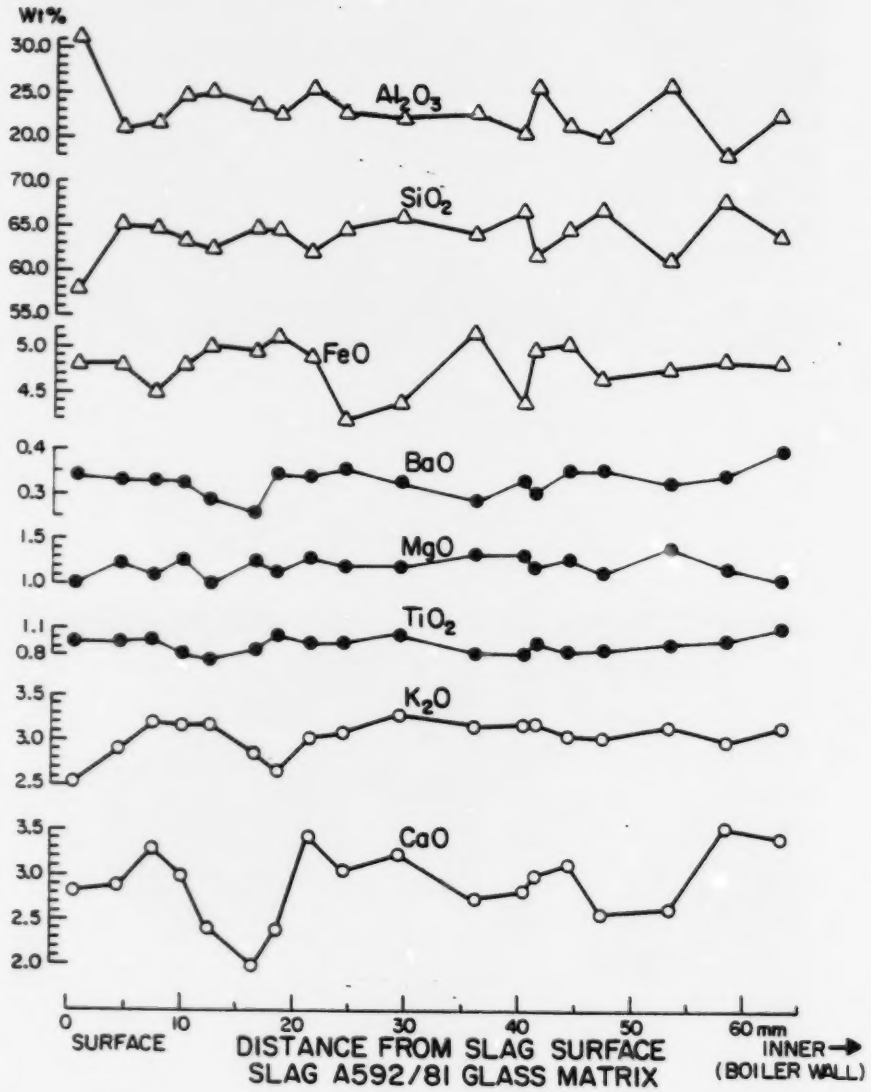

Fig. 22 - Compositional variation in glass matrix from the outer portion (near "liquid surface") to the inner portion (near boiler wall) of the slag A592/81. The analytical conditions are the same as those of slag A484/81.

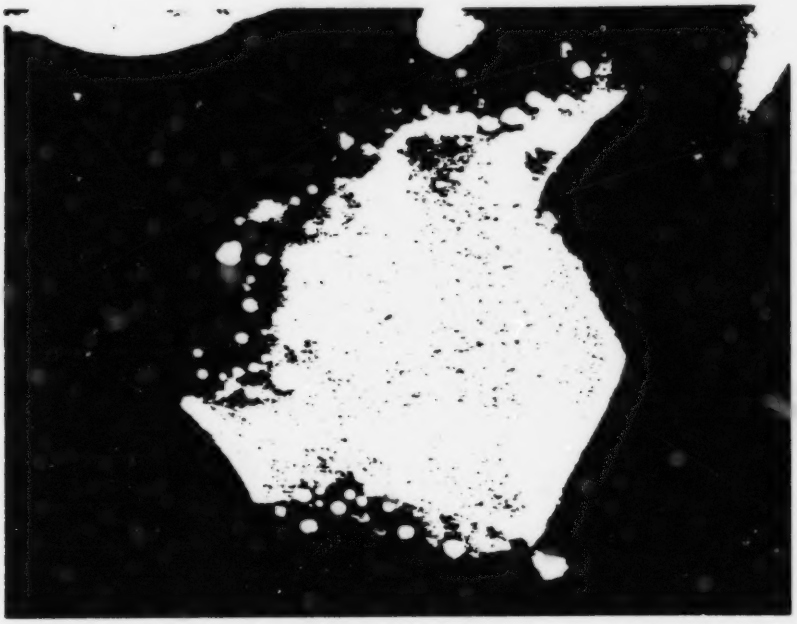

Fig. 23 - SEM photograph showing Fe_7Si_3 spherules (Si 16.4, Fe 81.3, P 2.1 wt %) in a fragment of slag A613/81. The matrix is glass.

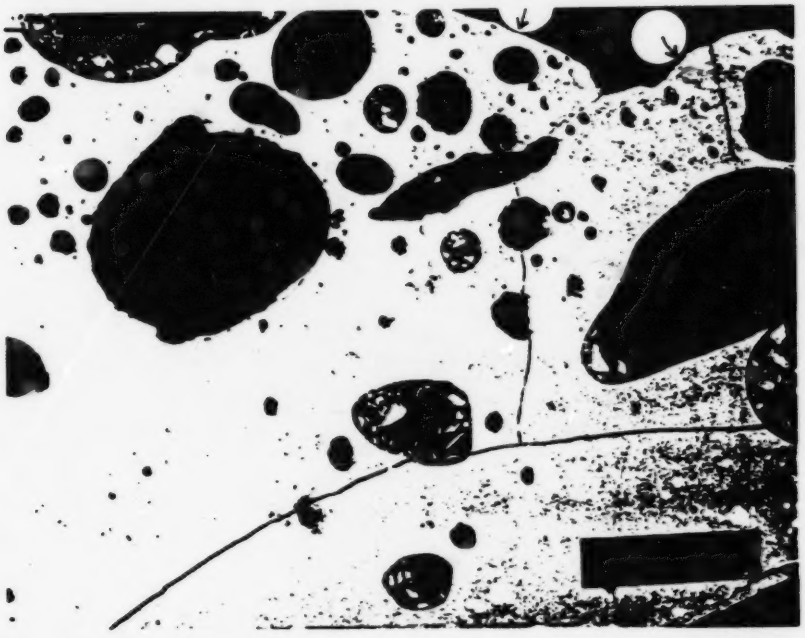

Fig. 24 - BSE image showing the general texture of the outermost portion (cross-section) of the slag A519/81. The uppermost surface-line represents the original liquid surface.

Fig. 25 - BSE image showing the general texture of the innermost portion of the slag A519/81. The details (a) is shown in Fig. 26.

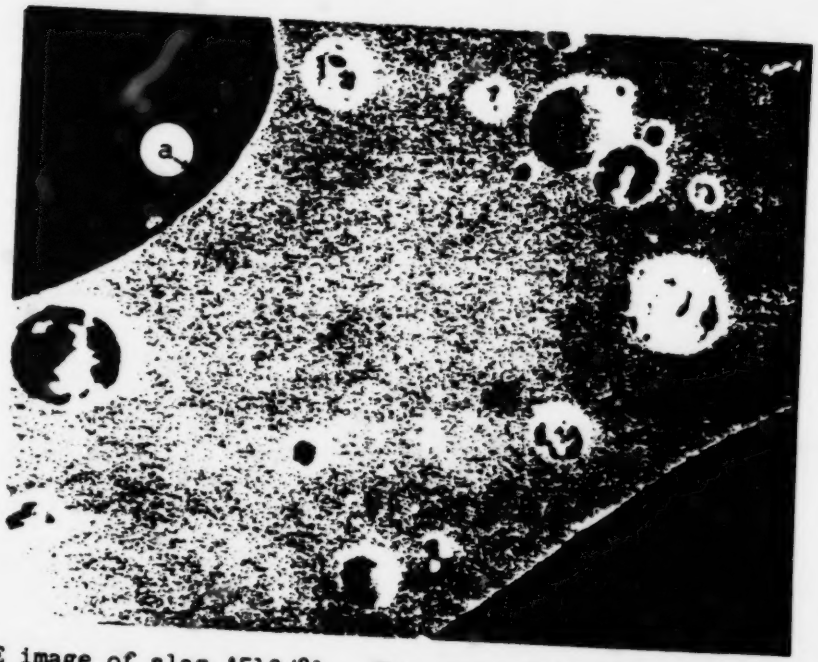

Fig. 26 - BSE image of slag A519/81. The compositional heterogeneity of the glass is evident from the variation of the brightness in the image. The darker areas have higher Al_2O_3. Spot (a) corresponds to the same in Fig. 25.

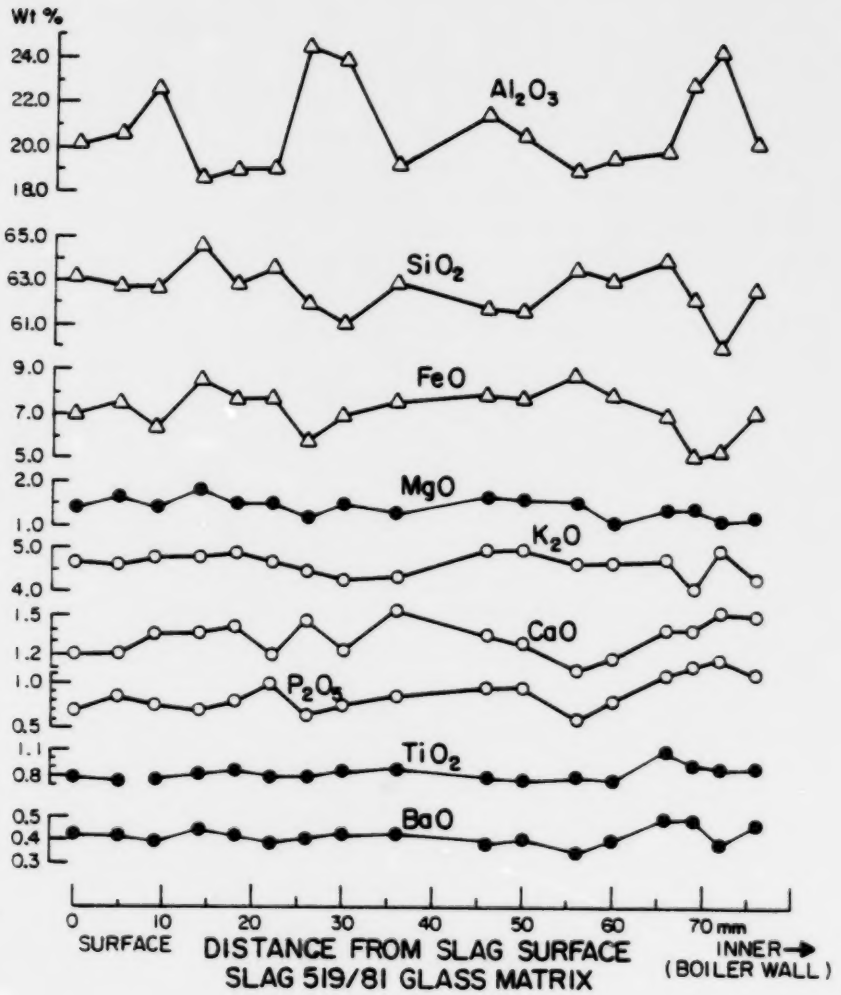

Fig. 27 - Compositional variation in glass matrix from the outer portion to the inner portion of the slag A519/81. The conditions of the analyses are the same as those of A484/81.

Fig. 28 - BSE image of a fragment of slag A519/81, showing the presence of iron oxide (a), SiO_2 (b), and mullite (c) in a matrix of glass.

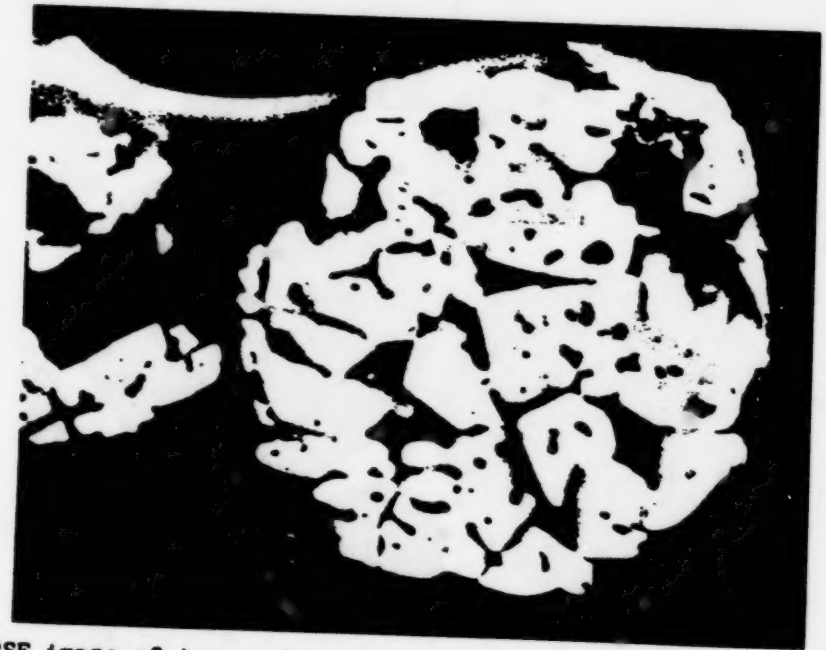

Fig. 29 - BSE image of iron oxide in slag A519/81, showing spherical aggregation of euhedral crystals.

Fig. 30 - BSE image showing the general texture of the outer portion of the slag A545/81.

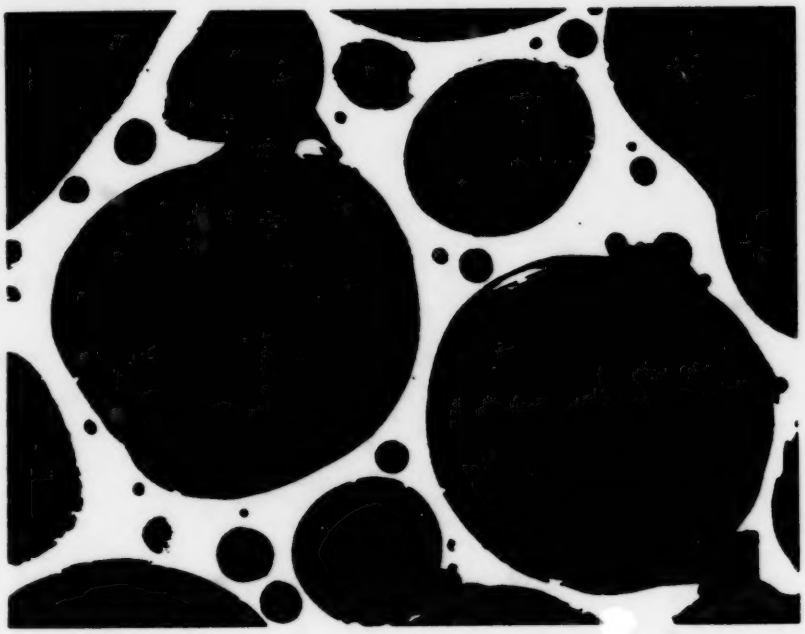

Fig. 31 - BSE image showing the general texture of the middle portion of the slag A545/81. The pore volume is more than the glass volume.

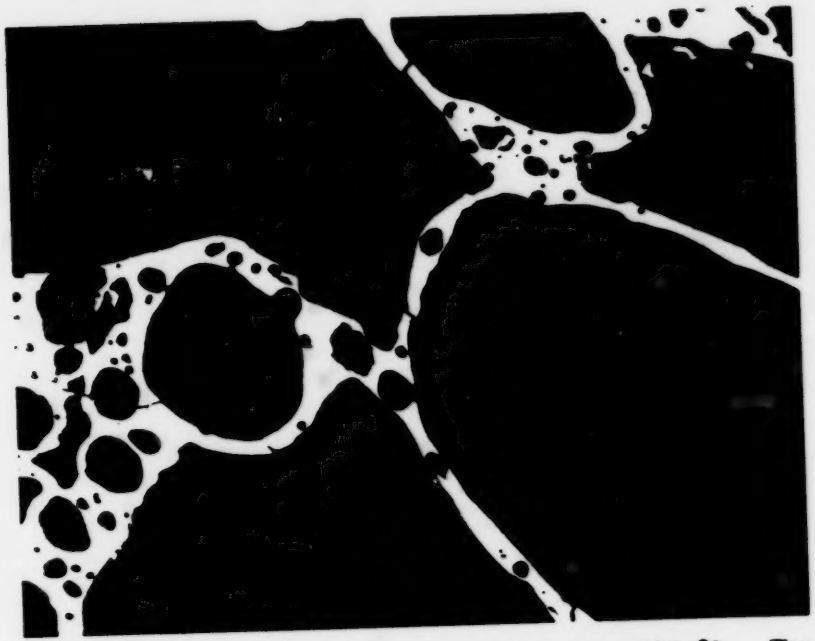

Fig. 32 - BSE image of the inner portion of the slag A545/81. The exceptionally large proportion of the pore volume in this photograph is a local feature, not representing the general texture of this portion.

Fig. 33 - BSE image of slag A545/81, showing heterogeneity of the glass composition. The darker areas contain more Al_2O_3.

POOR

QUALITY

ORIGINAL